Higher wavenumber shift of Pb (Al1/2Nb1/2)O3 substitution in relaxor ferroelectric Pb(Zr0.52Ti0.48)O3-Pb(Zn1/3Nb2/3)O3 ceramics

Zhu, J. J.; Li, C. Q.; Jiang, K.; Zhang, P.; Tong, W. Y.; Liu, A. Y.; Shi, W. Z.; Liu, Y.; Huang, Y. P.; Li, W. W.; Hu, Z. G.;

Originally published:

November 2016

Materials Letters 188(2017), 284-287

DOI: https://doi.org/10.1016/j.matlet.2016.10.110

Perma-Link to Publication Repository of HZDR:

https://www.hzdr.de/publications/Publ-24747

Higher wavenumber shift of $Pb(Al_{1/2}Nb_{1/2})O_3$ substitution in relaxor ferroelectric $Pb(Zr_{0.52}Ti_{0.48})O_3$-$Pb(Zn_{1/3}Nb_{2/3})O_3$ ceramics

Jiajun Zhu,[a,b] Chuanqing Li,[a,b] Kai Jiang,[a,b] Peng Zhang,[a] Wen-Yi Tong,[a,*], Aiyun Liu,[c] Wangzhou Shi,[c] Yu Liu,[d] Yi-Ping Huang,[e,*] Wenwu Li,[a,*] and Zhigao Hu[a]

[a] *Key Laboratory of Polar Materials and Devices, Ministry of Education, Department of Electronic Engineering, East China Normal University, Shanghai 200241, China*

[b] *National Laboratory for Infrared Physics, Shanghai Institute of Technical Physics, Chinese Academy of Sciences, Shanghai 200083, China*

[c] *Department of Physics, Shanghai Normal University, Shanghai 200234, China*

[d] *Helmholtz-Zentrum Dresden Rossendorf, Institute of Ion Beam Physics and Materials Research, Bautzner Landstrasse 400, D-01328 Dresden, Germany*

[e] *Department of Physics, Soochow University, Taipei 11102, Taiwan*

(Dated: Tuesday 1st November, 2016)

ABSTRACT

We report the lattice dynamics of $0.8Pb(Zr_{0.52}Ti_{0.48})O_3$-$(0.2\text{-}x)Pb(Zn_{1/3}Nb_{2/3})O_3$-$xPb(Al_{1/2}Nb_{1/2})O_3$ (0.8PZT-(0.2-x)PZN-xPAN, $0.02 \leq x \leq 0.08$) ceramics around morphotropic phase boundary (MPB) by infrared and Raman spectra. The dielectric functions in the wavenumbers range between 50 and 1000 cm^{-1} were extracted from the factorized oscillator model. The addition of PAN to PZT-PZN system introduces Al^{3+} ions to the B-site and all of these Raman-active modes in the measured range are related to B-site atoms vibration. The effect of PAN addition leads to infrared and Raman modes shifting to higher wavenumbers, because the atomic weight of Al is smaller than that of Zn. Therefore, the substitution of B-site atom in PZT-PZN system is the dominant reason to influence the frequency shift of infrared and Raman modes.

Keywords: PZT-based ceramics, Morphotropic phase boundary, Dispersion relation, Lattice vibrations, Raman spectroscopy.

*Corresponding authors. *E-mail addresses*: twy891137ssyy@163.com (W.-Y. Tong), yphuang@scu.edu.tw (Y.-P. Huang), wwli@ee.ecnu.edu.cn (W.W. Li).

1. Introduction

Relaxor ferroelectrics are technologically important transducer or actuator materials with extraordinary dielectric and electromechanical properties. [1] Because of their anomalous properties, relaxors have been a focus of intense attention, and comprehending the structure and dynamics of relaxors has been one of the long-standing fundamental scientific problem in solid state physics. [2–5] $Pb(Zn_{1/3}Nb_{2/3})O_3$ (PZN) is one of the most important relaxors among all the Pb-based relaxors, possessing excellent piezoelectric and dielectric properties. However, it is difficult to grow pure perovskite-type PZN ceramics by conventional oxide mixing methods, because the tolerance factor is low and the electronegativity difference between cations is small. It is an useful method to add other perovskite-type ferroelectrics to suppress the formation of pyrochlore phase. [6]

Among Pb-based ferroelectric, $Pb(Zr_xTi_{1-x})O_3$ (PZT) has been found to be one of the important materials with extremely large dielectric and piezoelectric properties near the region of morphotropic phase boundary (MPB) at x=0.52, due to the phase transition from tetragonal to rhombohedral via a bridging monoclinic phase. [7,8] Recent study of a single monoclinic phase in PZT ceramics shows that the extensional strain constant d_{33} is 520 pm/V and the transverse strain constant d_{31} is -200 pm/V, which are mainly attributed to the large intrinsic lattice instead of domain switching. [9] The dielectric, electric and piezoelectric properties of PZT can be improved by using dopants or forming a ternary system with the addition of Pb-based perovskite-type relaxor ferroelectrics. Forming a ternary system with the addition of PZN to PZT not only extends the stability region of the morphotropic phase boundary from one point to a line, but also lowers down the sintering temperature. The piezoelectric performance of PZT-PZN is higher than that of PZT. [10] X-ray diffraction, ferroelectric hysteresis and Raman measurements reveal that the MPB of xPZN-(1-x)PZT is between x=0.2 and x=0.3. [11] Electric properties and strain response are enhanced with the addition of $Pb(Al_{1/2}Nb_{1/2})O_3$ (PAN) in 0.2PZN-0.8PZT. [12] Moreover, the tetragonality decreases in coexistence of rhombohedral and tetragonal phase with the addition of PAN=0.02. Above PAN=0.05, the structure changes from MPB to single tetragonal phase. [12]

Raman and infrared (IR) spectroscopy are non-destructive technique, which can provide information about lattice vibrations and the position of the ions. Recent systematic study of Raman spectra

of PZT materials assign the phonon bands on both sides of MPB, without any direct evidence for a monoclinic symmetry. [13,14] Doping is an useful method to modulate the properties of ferroelectric materials. Raman scattering spectra show that the effect of doping transitional metal oxide Fe_2O_3 on PZT-PZN reduces the average energy of the B-O bonding and induces the phase transition from rhombohedral structure to tetragonal phase, shifting $A_1(2TO)$ mode to a high wavenumber and silent mode to a low wavenumber. [15] However, quantitative evaluation of phase coexistence in PZT-based relaxors with doping oxide by Raman spectroscopy is not an easy way, because Raman spectra of such ceramics are usually broad and structure is very complicated around MPB. Compared with the analysis of oxide doping effect, it is easier to analyze the influence of PAN substitution on the optical properties of PZT-PZN, because PAN has a similar perovskite structure to PZT and PZN. The addition of PAN to PZT-PZN introduces Al^{3+} ions to the B-site, while Raman scattering and IR reflectance spectra are very useful techniques to detect the B-site ordering degree.

In this letter, we investigate the influence of PAN in lattice vibrations of PZT-PZN ceramics by combining IR reflectance spectra with Raman scattering. Factorized oscillator model is used to better understand the IR spectra, to assign the mode symmetries, and to express the dielectric functions. Effects of PAN concentration on frequencies of both Raman-active and IR-active phonon modes have been discussed in detail.

2. Experimental procedure

Ferroelectric PZT-PZN-PAN ceramics were grown using traditional solid-state reaction sintering method. [12] The nominal concentration of $0.8Pb(Zr_{0.52}Ti_{0.48})O_3$-$(0.2\text{-}x)Pb(Zn_{1/3}Nb_{2/3})O_3$-$xPb(Al_{1/2}Nb_{1/2})O_3$ (0.8PZT-(0.2-x)PZN-xPAN) ceramics was x from 0.02 to 0.08. The near-normal incident ($\sim 10^\circ$) far-infrared (FIR) reflectance measurements were performed from 50 to 1000 cm^{-1} using a Bruker VERTEX 80 V Fourier transform infrared spectrometer. The spectral resolution was 2 cm^{-1} and 4 cm^{-1} in the low- and high-frequency ranges, respectively. Different beamsplitters of optimized KBr or 6-μm thick mylar were used with room temperature DLaTGS detector or deuterated triglycine sulfate (DTGS) detector for each IR region. Gold mirror was taken as reference for spectra in the whole region. Raman spectra were recorded by a Jobin-Yvon LabRAM HR 800 spectrometer with a He-Ne laser as the excited light, which was operated at a wavelength of 632.8nm.

The laser beam was focused through a 100× microscope and dispersed by a 1800 g/mm grating.

3. Results and discussions

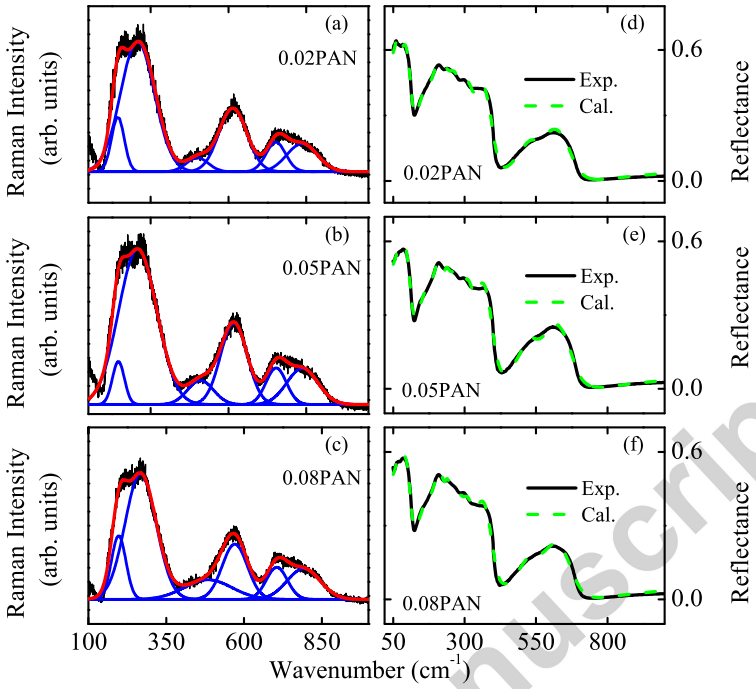

Figure 1: (a) Raman spectra of PZT-PZN-0.02PAN, (b) PZT-PZN-0.05PAN, and (c) PZT-PZN-0.08PAN ceramics at room temperature. The experimental (solid lines) and calculated (dashed lines) infrared reflectance spectra of (d) PZT-PZN-0.02PAN, (e) PZT-PZN-0.05PAN, and (f) PZT-PZN-0.08PAN ceramics, respectively.

Raman scattering is an effecitve method for the investigation of local lattice distortions on an atomic scale. Figs. 1(a)-1(c) show Raman spectra of PZT-PZN-PAN ceramics, which are fitted with Gaussian lineshape to extract the phonons frequencies. These vibration bands of PZT-PZN-PAN ceramics are wider and more dispersive than those of PZT, [13] because the formation of PZT-PZN-PAN systems enhances the disorder in B-site ions. The broad bands at 195 and 260 cm^{-1} are attributed to BO_6 rotation and B-localized vibration mode, respectively. The weak peak near 460 cm^{-1} is assigned to O-B-O bending vibrations. The peak observed in the high-frequency regions at 570 cm^{-1} is characteristic of perovskites with different B cations and is assigned to O-B-O bending mode. The modes at 700 and 790 cm^{-1} arise from the B-O stretching modes. [16–19] These modes are activated by the inequivalency of Al, Nb, Zn, Ti cations that occupy the B site of the perovskite cell. Table 1 lists Raman-active mode of PZT-PZN-PAN ceramics. With the addition of PAN, all

Table 1. The phonon mode frequencies of the PZT-PZN-PAN ceramics are extracted from the Gauss curve fitting (Fig. 1).

Raman mode	0.02PAN	0.05PAN	0.08PAN	Vibration mode
$E(2TO_1)$	195	196	197	BO_6 rotation
Silent $E+B_1$	258	259	268	B-localized
$E(2LO)$	450	460	484	O-B-O bending
$A_1(4TO)$	564	567	570	O-B-O bending
$E(4LO)$	702	703	705	B-O stretching
$A_1(3LO)$	787	788	792	B-O stretching

the Raman-active modes shift to higher wavenumbers due to the lighter Al mass than Zn mass. All of these Raman-active modes are related to B-site atoms so the substitution of B-site atom is the dominant reason to influence Raman shift.

IR reflectivity spectra were fitted using the factorized oscillator model of the dielectric function, $\varepsilon(\nu)=\varepsilon_\infty\prod_{j=1}^{n}\frac{\nu_{\mathrm{LO}_j}^2-\nu^2+i\nu\gamma_{\mathrm{LO}_j}}{\nu_{\mathrm{TO}_j}^2-\nu^2+i\nu\gamma_{\mathrm{TO}_j}}$, where the dielectric function is related to reflectivity R(ν) by $\mathrm{R}(\nu)=|\frac{\sqrt{\varepsilon(\nu)}-1}{\sqrt{\varepsilon(\nu)}+1}|^2$. ε_∞ is the high frequency constant, ν_{TO_j} and ν_{LO_j} are transverse optic (TO) and longitudinal optic (LO) frequency of the jth mode, respectively, and γ_{TO_j} and γ_{LO_j} are the corresponding damping constants. Experimental and fitting IR reflectance spectra of PZT-PZN-PAN ceramics are shown in Figs. 1(d)-1(f). Solid lines are experimental data, and dashed lines are fitting results with the factorized oscillator model. One can see that all spectra show similar behavior, which corresponds to the addition of PAN, because small PAN content difference slightly influences the phonon broadening and frequency.

The real and imaginary parts of dielectric function obtained from the fits of IR reflectivity are shown in Fig. 2. Three main bands in the reflectivity of PZT-PZN-PAN ceramics can be observed. They are related to three TO modes. Correspondingly, Fig. 3 shows the positions of the three LO bands in the imaginary part of the inverse permittivity. Low frequency $E(\mathrm{TO}_1)$ mode leads to the strong increase of real part of the dielectric function below 100 cm^{-1}, which is observed in other ferroelectrics as well. [17–20] The IR reflectivity spectra of several Pb-based relaxors can be well compared due to their similarity in many aspects. The dielectric response is dominated by the lowest

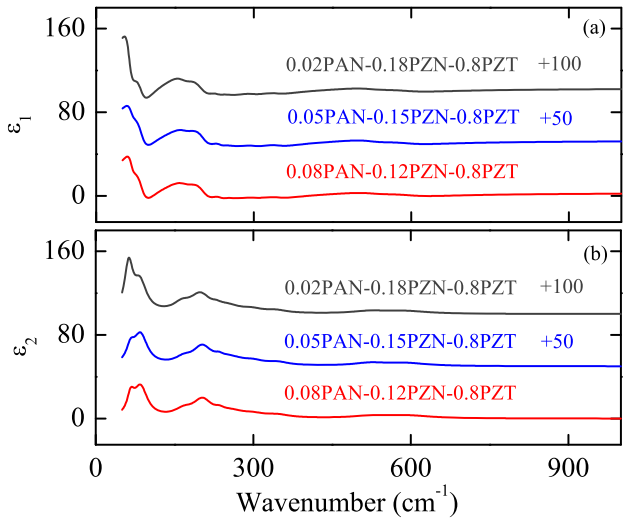

Figure 2: (a) Real and (b) imaginary parts of the dielectric function of PZT-PZN-PAN ceramics.

frequency phonon mode, related to Pb-BO_3 (B=Zr, Nb, Al, Ti) vibration. The simple cubic ABO_3 perovskite structure $PbTiO_3$, $BaTiO_3$, and $KNbO_3$ were reported to have three triply degenerate zone-centre IR active modes of the same symmetry ($3F_{1u}$) as well. [17] In each eigenmode, all the ions are vibrating along the mode dipole moment. These three modes are the so-called Last mode, Slater mode, and Axe mode, which represent the oscillation of A-cations against the BO_6-octahedra framework, mutual B-rigid O_6 oscillations, and the bending of the O_6 octahedra, respectively. The Last-type band locates at lowest frequencies, leading a relatively large contribution to the static dielectric constant. Appearance of the spontaneous polarisation along one of the cubic axes splits each of the three F_{1u} triplet modes in an A_1-E pair. The modes belonging to A_1 and E symmetry types contribute to distinct components of the dielectric tensor parallel and perpendicular to the spontaneous polarization, respectively.

The weak band around 300 cm^{-1} corresponds to the stretching mode originated from the B-site ordering, and the band around 350 cm^{-1} is due to the geometric resonance associated with the splitting of LO_2 mode. Similar band at about 65 cm^{-1} stretching mode was reported in most of the lead-based perovskites including PZT and PZN-based systems as well. [18, 19] The parameters of these fits are listed in Table 2 for the frequencies and damping of the LO and TO modes. With the addition of PAN, the frequencies of all the IR-active phonon modes increase because the atomic weight of Al (26.98) is smaller than that of Zn (65.38). The substitution Al for Zn causes the lattice

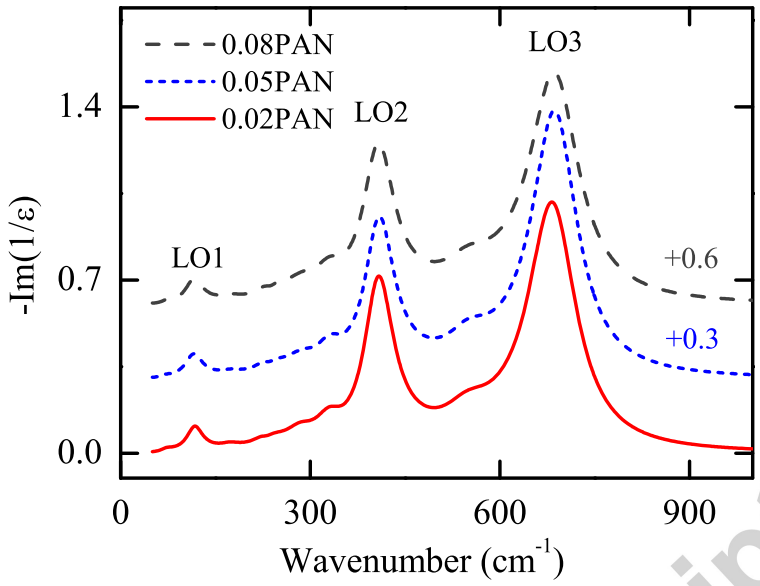

Figure 3: Imaginary parts of the inverse permittivity of PZT-PZN-PAN ceramics.

shrinkage, resulting in the shifts of the phonon frequencies to higher wavenumbers. It is in good agreement with Raman data, indicating that two analysis methods agree consistently.

4. Conclusions

In summary, the lattice vibration of PZT-PZN-PAN ceramics was studied by IR and Raman spectra. The dielectric functions were extracted from the factorized oscillator model. It was found that with the addition of PAN, the frequencies of IR and Raman modes shift to higher wavenumbers due to the smaller atomic weight of Al than that of Zn.

Table 2. Frequencies ω and damping parameters γ of the phonon modes in PZT-PZN-PAN ceramics obtained from the fit of the infrared reflectivity spectra. ϵ_∞=3. The unit is cm^{-1}.

	0.02PAN				0.05PAN				0.08PAN			
No.	ω_{TOi}	γ_{TOi}	ω_{LOi}	γ_{LOi}	ω_{TOi}	γ_{TOi}	ω_{LOi}	γ_{LOi}	ω_{TOi}	γ_{TOi}	ω_{LOi}	γ_{LOi}
1	63.5	18.7	85.7	30.7	66.9	19.1	86.7	32.3	67.2	16.7	86.9	31.8
2	165	39.6	230.2	20.6	168.2	40	234.9	19.6	168.7	42.8	235.4	18.5
3	200.2	47.5	252.6	60.7	204	44	257.8	65.2	204.2	43.8	258.2	68.2
4	298.2	52.4	344.3	50.4	301.2	50.3	347.4	50.4	302	54.3	347.5	54.2
5	523.8	80.6	591.5	107.5	523.9	78.3	592.4	103.5	526.6	84.3	596.5	108.5

Acknowledgment

This work was supported by CSC-DAAD postdoctoral scholarship (CSC No. 201500110019 and DAAD No. 57165010) funded by CSC and Deutscher Akademischer Austauschdienst, Shanghai Sailing Program funded by STCSM (Grant No. 15YF1413900), NSFC of China (Grant No. 61504043), the International Postdoctoral Exchange Fellowship Program (Grant No. 20150057) and Project funded by China Postdoctoral Science Foundation (Grant No. 2014M560357).

References

[1] S.E. Park, T.R. Shrout, J. Appl. Phys. 82 (1997) 1804-1811.

[2] H. Takenaka, I. Grinberg, A.M. Rappe, Phys. Rev. Lett. 110 (2013) 147602-1-5.

[3] S. Zhang, F. Li, X. Jiang, J. Kim, J. Luo, X. Geng, Prog. Mater. Sci. 68 (2015) 1-66.

[4] J.J. Zhu, J.Z. Zhang, K. Jiang, H.W. Zhang, Z.G. Hu, H.S. Luo, J.H. Chu, J. Am. Ceram. Soc. 99 (2016) 2408-2414.

[5] Y.H. Paik, H.S. Kojori, J.H. Yun, S.J. Kim, Mater. Lett. 185 (2016) 247-251.

[6] R.A. Cowley, S.N. Gvasaliya, S.G. Lushnikov, B. Roessli, G.M. Rotaru, Adv. Phys. 60 (2011) 229-327.

[7] B. Noheda, J.A. Gonzalo, L.E. Cross, R. Guo, S.E. Park, D.E. Cox, G. Shirane, Phys. Rev. B 61 (2000) 8687-8695.

[8] F.F. Abdullah, A. Nemati, R. Bagheri, Mater. Lett. 151 (2015) 85-88.

[9] L.L. Fan, J. Chen, Y. Ren, Z. Pan, L.X. Zhang, X.R. Xing, Phys. Rev. Lett. 116 (2016) 027601-1-5.

[10] M.P. Zheng, Y.D. Hou, F.Y. Xie, J. Chen, M.K. Zhu, H. Yan, Acta Mater 61 (2013) 1489-1498.

[11] N. Vittayakorn, G. Rujijianagul, X. Tan, H. He, M.A. Marquardt, D.P. Cann, J. Electroceram. 16 (2006) 141-149.

[12] L.L. Wei, A.Y. Liu, C.C. Jin, F.T. Lin, P. Wang, Q.R. Yao, C.Y. Tian, Y. Li, J. Tang, H.L. Han, W.Z. Shi, C.B. Jing, J. Alloy Compd. 590 (2014) 368-372.

[13] E. Buixaderas, I. Gregora, M. Savinov, J. Hlinka, L. Jin, D. Damjanovic, B. Malic, Phys. Rev. B 91 (2015) 014104-1-9.

[14] Q. Wan, Q.R. Gu, J. Xing, J. Chen, Mater. Lett. 92 (2013) 52-56.

[15] M. Zheng, Y. Hou, S. Wang, C. Duan, M. Zhu, H. Yan, J. Am. Ceram. Soc. 96 (2013) 2486-2492.

[16] B. Noheda, D.E. Cox, Phase Transit. 79 (2006) 5-20.

[17] J. Hlinka, J. Petzelt, S. Kamba, D. Noujni, T. Ostapchuk, Phase Transit. 79 (2006) 41-78.

[18] E. Buixaderas, D. Nuzhnyy, J. Petzelt, L. Jin, D. Damjanovic, Phys. Rev. B 84 (2011) 184302-1-12.

[19] J. Macutkevic, S. Kamba, J. Banys, A. Brilingas, A. Pashkin, J. Petzelt, K. Bormanis, A. Sternberg, Phys. Rev. B 74 (2006) 104106-1-10.

[20] R. Loudon, Adv. Phys. 50 (2010) 813-864.